Summary of a Simulation of the ANITA Detector

Amy Connolly

December 15, 2011

Abstract

We outline our code written to simulate the ANITA detection system.

Contents

1 Introduction

The code outlined here is meant to be a simulation of the ANITA and ANITA-lite detection systems. It should provide the collaboration with a tool to study the impact of various effects on the experiment's sensitivity. It will also provide the energy-dependent sensitivity that will be used for setting limits on models for UHE neutrinos from ANITA-lite data and ultimately from the full ANITA flights. It also serves as a consistency check with the Monte Carlo simulation being developed by our collaborators at the University of Hawaii.

2 Overall Strategy

The simulation models interactions from neutrinos of a specified energy. The Askaryan pulse is parameterized by the current theoretical model. We require an interaction to occur within the Antarctic ice volume within the balloon's horizon. We generate two different types of events. The first is where the ray seen by the balloon is direct; the ray is emitted from the interaction upward. The second is where the ray is emitted downward and is reflected from the ice-rock interface before being reaching the surface. For half of the neutrinos, we force the ray to be the first type and for the other half, the second type. For a given type of ray, we find the unique path along which an RF signal would travel from the interaction to the balloon, snelled through ice layers at the ice-air surface. Next, we pick a direction for the neutrino path, only considering directions such that the Cerenkov cone is close enough to the unique ray from interaction to balloon that the signal is still detectable under a best-case scenario. Depth-dependent attenuation lengths and indices of refraction in the ice are based on recent South Pole measurements. Surface slopeyness is taken into account under a simple model. Frequency-dependent antenna response is based on the manufacturer's specifications. The trigger configuration is based on the most current design. The restrictions in neutrino phase space that come about in our selection of neutrino interaction positions and neutrino directions are corrected for in the final calculation (see Section 7).

2.1 Coordinate System

Where Cartesian coordinates are used, we define x,y and z to be zero at the center of the earth. The $+z$ axis runs from the center of the earth to the south pole (so, our coordinate system is defined so that the earth is "upside-down"). The x and y axes lie in the 0° latitude plane, with $+x$ pointing to the 90° E longitudinal line, and $+y$ points to 0° longitude. This coordinate system is right-handed.

The ϕ coordinate is defined as usual, zero along the $+x$ axis, and increasing moving counter-clockwise from the view looking down on the $+z$ axis. The θ coordinate is measured relative to the $+z$ axis.

Bedrock and ice surface elevations are measured radially from the center of the earth, and are quoted relative to sea level. Sea level $r(\theta)$ is latitude-dependent and is quoted as a distance from the center of the earth. We use a geoid shape given by [9]:

$$r(\theta) = \frac{r_{min} \cdot r_{max}}{\sqrt{r_{min}^2 - (r_{min}^2 - r_{max}^2)\cos^2\theta}} \tag{1}$$

where $r_{min} = 6356.752$ km and $r_{max} = 6378.137$ km.

To accommodate the global crust model 2.0 [2] for thicknesses of sediment layers through the crust as well as ice thicknesses, which is on a $2° \times 2°$ grid, we bin the earth's surface into

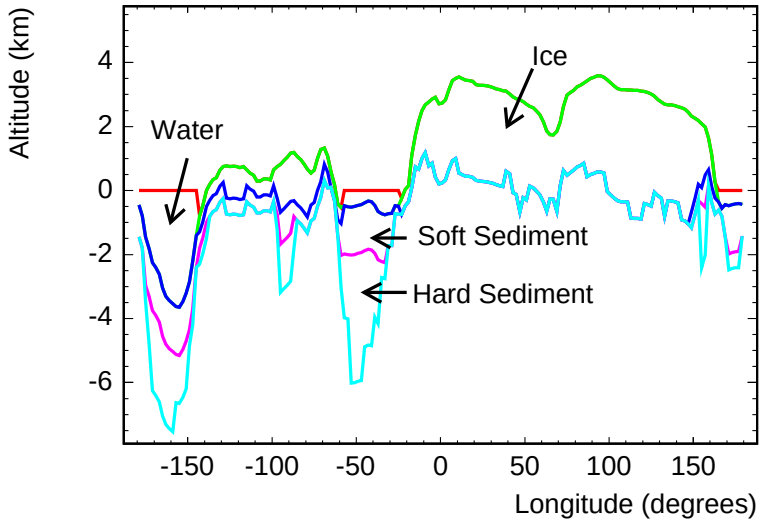

Figure 1: Altitude of the upper four layers given in Crust 2.0 along the the 75° S latitude line. The horizontal axis is degrees in longitude.

180 bins in longitude and 90 bins in latitude. Note that the resulting bins are not uniform in area. The bins in latitude are numbered such that the 0^{th} bin is closest to the $+z$ axis (at the south pole), and the 89^{th} bin is closest to the north pole ($-z$).

2.2 CSEDI Crust 2.0

Crust 2.0 is the latest model of the Earth's interior near the surface published as the result of an initiative called Cooperative Studies of the Earth's Deep Interior (CSEDI). It is based on seismological data, and the model gives thicknesses and densities of each of seven layers in $2° \times 2°$ bins: ice, water, soft sediments, hard sediments, upper crust, middle crust, and lower crust. The ice thicknesses in Crust 2.0 are claimed to be within 250 m of the true ice thickness. Sediment thicknesses in each cell are to within 1.0 km of the true sediment thickness and crustal thickness are within 5 km of the true crustal thicknesses.

Figures 1 and 2 show the elevations of the seven crustal layers included in Crust 2.0.

We compute the total Antarctic ice volume by summing the product of ice thickness and surface area for each bin within the Antarctic continent. For the area of each bin, we use:

$$\int_{\phi_1}^{\phi_2} \int_{\theta_1}^{\theta_2} \sin\theta \; d\theta \; d\phi = (\phi_1 - \phi_2) \times (\cos\theta_1 - \cos\theta_2) \tag{2}$$

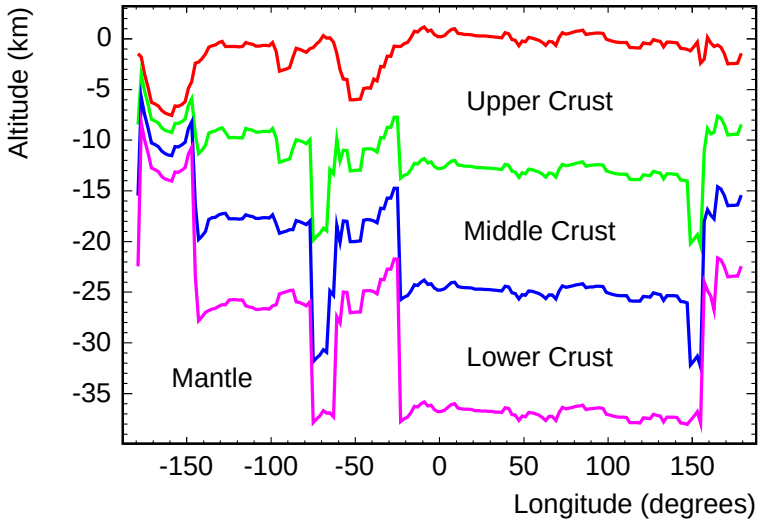

Figure 2: Altitude of the lower three layers given in Crust 2.0 along the the 75° S latitude line.

Where the limits of the integrals define the edges of the bin in latitude and longitude. We find 2.7×10^{16} m^2 of Antarctic ice in this model. Compare this to the 3.01098×10^{16} m^3 volume of ice in Antarctica reported by the US Geological Survey [11]; they are different by 10%. Unfortunately, Crust 2.0 calls any ice that sits above water (ice shelves) just water. Therefore, the Ross Ice Shelf needs to be added into the model by hand. Ice shelves make up 2.4% of the ice volume in Antarctica, so it won't account for the entire 10% difference.

3 The Askaryan Signal

3.1 Magnitude of the Pulse

We use the parameterization outlined in [6] for the peak of the Askaryan signal:

$$\frac{\mathcal{E}^{(@1\mathrm{m})}}{\mathrm{V/m/MHz}} = 2.53 \times 10^{-7} \cdot \frac{\sin\theta_v}{\sin\theta_c} \cdot \frac{E_{em}}{\mathrm{TeV}} \cdot \frac{\nu}{\nu_0} \cdot \frac{1}{1. + \left(\frac{\nu}{\nu_0}\right)^{1.44}} \tag{3}$$

where ν is the frequency, $\nu_0 = 1.15$ GHz, E_{em} is the shower energy, θ_v is the viewing angle and θ_c is the Cerenkov angle.

3.2 Electromagnetic and Hadronic Components of the Shower

We assume flavor democracy; that by the time the neutrinos get here, the flavors are fully mixed. We also keep track of each flavor individually so the sensitivity to each flavor may be quoted separately.

We pick an inelasticity y according to [7], which we have approximated by a double-exponential. If we call the electromagnetic component f_e and the hadronic component f_h, then the dependence of f_e and f_h on y depends on the whether it is a charged current interaction that occurred or a neutral current interaction. We choose 70.64% of the events at random to be charged-current and the remainder to be neutral current. If the incident neutrino was a ν_e and it is a charged current event, then $f_e = 1 - y$ and $f_h = y$. If the incident neutrino was ν_τ or ν_μ, or if the ν_e interacts through a neutral current, then the electromagnetic component is for now treated as negligible, and $f_h = y$. A future version of the code will include μ/τ bremsstrahlung and photo-nuclear interactions.

3.3 Width of Cerenkov Cone

The user can select one of two different parameterizations of the width of the Cerenkov cone in inputs.txt. Here we refer to the two parameterizations as the "old" parameterization and "new" parameterization, for lack of a better terminology. The user should select 0 (1) for the old (new) parameterizations in the appropriate line in the inputs.txt file. In both parameterizations, the width of the Cerenkov cone is different for the electromagnetic and hadronic components of the shower.

3.3.1 Old Parameterization

For this parameterization, we model the cone widths as described in [12] for electromagnetic showers and and in [13] for hadronic showers.

The width of the electromagnetic component in degrees is characterized by:

$$\Delta\theta_{em}(\nu) = 2.7 \cdot \frac{\nu_0}{\nu} \cdot \left(\frac{E_{LPM}}{0.14E_\nu + E_{LPM}}\right)^{0.3} \tag{4}$$

where E_{LPM} is energy above which the LPM effect becomes important. The LPM effect causes the bremsstrahlung interaction to become suppressed because the momentum transfer ($\propto k/E^2$) becomes so small that the Heisenberg uncertainty causes the interaction to occur over many scattering centers, resulting in destructive interference. This effect reduces the width of the Cerenkov cone, but not the magnitude of the electric field at the Cerenkov angle. For E_{LPM}, we use [4]:

$$E_{LPM} = 2 \times 10^{15} \frac{\chi_{\text{medium}}}{\chi_{\text{ice}}} \tag{5}$$

where $\chi_{\text{ice}} = 39.5$ cm is the radiation length of ice and χ_{medium} is the radiation length of the medium of interest.

The radio pulse from the hadronic component of the shower is parameterized as in [13], defining $\epsilon = \log_{10} E_\nu / 1\text{TeV}$:

$$\Delta\theta_{had} = \tfrac{\nu_0}{\nu} \cdot (2.07 - 0.33 \cdot \epsilon + 0.075 \cdot \epsilon^2) \qquad \epsilon \geq 0 \text{ and } \epsilon < 2 \tag{6}$$

$$\Delta\theta_{had} = \tfrac{\nu_0}{\nu} \cdot (1.744 - 0.0121 \cdot \epsilon) \qquad 2 \leq \epsilon < 5 \tag{7}$$

$$\Delta\theta_{had} = \tfrac{\nu_0}{\nu} \cdot (4.23 - 0.785 \cdot \epsilon + 0.055 \cdot \epsilon^2) \qquad 5 \leq \epsilon < 7 \tag{8}$$

$$\Delta\theta_{had} = \tfrac{\nu_0}{\nu} \cdot (4.23 - 0.785 \cdot 7.0 + 0.055 \cdot 7.0^2) \cdot [1.0 + (\epsilon - 7.0) \cdot 0.075] \qquad \epsilon \geq 7 \tag{9}$$

According to [6], the angular distribution of the radio pulse is expected to exhibit a diffraction pattern centered at the Cerenkov angle. However, for now we approximate the shape of the electromagnetic or hadronic pulse with a double Gaussian distribution with standard deviations given by $\Delta\theta_{em}$ and $\Delta\theta_{had}$.

In this "old" parameterization, the signal strength at viewing angle θ away from the Cerenkov angle θ_C is given as in [12] and [13]:

$$E(\theta) = \frac{\sin\theta}{\sin\theta_C} \cdot E(\theta_C) \cdot \exp\left[-\ln 2 \left(\frac{\theta - \theta_C}{\Delta\theta_{\text{em,had}}} \right)^2 \right] \tag{10}$$

3.3.2 New Parameterization

For this parameterization, we model the cone widths guided by [14].

Electromagnetic showers in ice are modelled just as described in the previous section, but here we allow for the possibility of scaling width for other media, in case one would like to use this same code for a detector in salt, for example. We use Equation 4 for the cone width for the electromagnetic component of the shower and then scale for other media, inspired by Equation 9 in [14], according to:

$$\Delta\theta_{\text{em,medium}} = \Delta\theta_{\text{em,ice}} \cdot \frac{\rho_{\text{medium}}}{\rho_{\text{ice}}} \cdot \frac{\text{K}_{\Delta,\text{medium}}}{\text{K}_{\Delta,\text{ice}}} \cdot \frac{n^2_{\text{medium}} - 1}{n^2_{\text{ice}} - 1} \tag{11}$$

Hadronic showers are modelled as laid out in Equation 9 in [14]:

$$\Delta\theta_{\text{had,medium}} = \frac{c}{\nu} \cdot \frac{\rho_{\text{medium}}}{\rho_{\text{ice}}} \cdot \frac{\text{K}_{\Delta,\text{medium}}}{\text{K}_{\Delta,\text{ice}}} \cdot \frac{n^2_{\text{medium}} - 1}{n^2_{\text{ice}} - 1} \tag{12}$$

In this "new" parameterization, the signal strength at viewing angle θ away from the Cerenkov angle θ_C is given as in [14]:

$$E(\theta) = \frac{\sin\theta}{\sin\theta_C} \cdot E(\theta_C) \cdot \exp\left[-\left(\frac{\theta - \theta_C}{\Delta\theta_{\mathrm{em,had}}}\right)^2\right] \tag{13}$$

3.4 Additional factor of root 2/2

4 Event Geometry

4.1 Picking Interaction Point and Direction

We force the neutrino interaction to occur within the balloon's horizon, given the balloon position for that event. Within that horizon, we stack the ice thicknesses of all of the bins in longitude and latitude. The height of each bin in the stack is the difference between the ice surface and soft sediment elevations for that bin, which is the ice thickness. We pick a random point along the height of the stack to determine which bin the interaction occurs in, and at what elevation within that bin. The exact position of the interaction in the longitudinal and latitudinal directions is chosen at random within the bin. The position of the interaction is denoted here as $\vec{x}_{int}$. (wufan.From $\vec{(}x)_(int)$ we get the mirror position of the interaction below the local bottom of the ice where we assume the local bottom of the ice is an approximately flat mirror.)

The event is then given a weight d_i^{pos} that is the volume of ice within the horizon divided by the total volume of ice in Antarctica. The volume of ice for each balloon position (in 100 discrete bins) is calculated once at the beginning of the code so that it does not need to be calculated for each event.

The event is rejected if the interaction-to-balloon ray traverses rock. Since this is essentially the same as requiring that the balloon be within the horizon, it would never reject an event if it weren't for surface tilt and the fact that we generate events to just beyond the horizon to be safe.

We pick a neutrino direction at random in $\cos\theta$ and ϕ. It is denoted here as $\vec{n}_\nu$. The neutrino momentum (non-normalized) is denoted $\vec{p}_\nu$ and its magnitude simply p_ν. If we choose θ and ϕ among all possibilities, the interaction-to-balloon ray may be far enough off of the Cerenkov cone that the signal is undetectable, even if all other conditions are ideal. Therefore, we only generate neutrino directions such that $|\theta_{\nu,ice} - \theta_c| < \theta_{th}$ where $\theta_{\nu,ice}$ is the angle between the neutrino direction($\vec{n}_\nu$) and (wufan the ray out from the interaction point in the ice($\vec{n}_{ray}$). For direct rays $\vec{n}_{ray}$ is the direction of interaction-to-balloon ray,but for reflected rays it is the mirror vector of the mirror_interaction_point-to-balloon, which means

here $\vec{n}_{ray}$ is downward).) The Cerenkov angle $\theta_c = \mathrm{Cos}^{-1}(1/\mathrm{n})$, see Section 5.2 for how the index of refraction is chosen. The angle θ_{th} is the maximum angle that the ray may diverge from the center of the Cerenkov cone for the interaction to still be detectable, given the parameters of the event.

To find θ_{th}, first we find the maximum electric field (in V/m/MHz) at 1 m that is possible to be emitted from the interaction within the antenna bandwidth using Equation 3. For $\mathcal{E}^{(@1\mathrm{m})} = \mathcal{E}^{(@1\mathrm{m})}{}_{max}$, we take $\nu = \nu_{max} = 1200$ MHz. Here, we use $\sin\theta_v = 1$ since it is the most conservative value and it allows us to solve for $\Delta\theta_{th} = \theta_v - \theta_c$. Then, we account for the distance between the interaction and payload r by dividing that distance into $\mathcal{E}^{(@1\mathrm{m})}{}_{max}$ to get the maximum electric field possibly seen at the payload, $\mathcal{E}_{max}$. From $\mathcal{E}_{max}$, we derive θ_{th}.

When the shower is dominated by either electromagnetic or hadronic energy deposition, the angular threshold (the angle beyond which the signal could not possibly be detectable) is found by solving for $\Delta\theta_{th}$ in the equation:

$$\begin{aligned} V_{noise}^{max} \cdot N_\sigma &= f_{em} \cdot \mathcal{E}^{(@1\mathrm{m})}{}_{max}(\sin\theta_v = 1) \cdot h_{eff}^{max} \cdot B \\ &\quad \cdot \exp\left(-\tfrac{1}{2} \cdot \tfrac{\Delta\theta_{\mathrm{th}}^2}{\Delta\theta(\mathrm{max})_{\mathrm{em}}^2}\right) \qquad f_{em} \gg f_{had} \qquad (14) \\ &= f_{had} \cdot \mathcal{E}^{(@1\mathrm{m})}{}_{max}(\sin\theta_v = 1) \cdot h_{eff}^{max} \cdot B \\ &\quad \cdot \exp\left(-\ln 2 \cdot \tfrac{\Delta\theta_{\mathrm{th}}^2}{\Delta\theta(\mathrm{max})_{\mathrm{had}}^2}\right) \qquad f_{had} \gg f_{em} \qquad (15) \end{aligned}$$

Here, $f_{em,had}$ is the EM or hadronic fraction, if only one of them is non-negligible (otherwise, see the next paragraph). The maximum effective height h_{eff}^{max} of the antennas over the antenna bandwidth is 63 cm (from the antenna specs). The width of one bandwidth slice within the larger antenna bandwidth is denoted B. The variables $\Delta\theta(\mathrm{max})_{\mathrm{em,had}}$ are the maximum widths of the Cerenkov cone due to the electromagnetic and hadronic showers over the bandwidth available to the antennas. Section 3.3 describes how these widths are determined. The largest widths are at the lowest frequency, 200 MHz; we find $\theta(\mathrm{max})_{\mathrm{had}} = 3.7^\circ$ and $\theta(\mathrm{max})_{\mathrm{em}} = 1.1^\circ$ for deep ice, higher within the firn (see Section 3.3). V_{noise}^{max} is the maximum expected noise level in a single bandwidth slice among the 4 layers of antennas, given their cant angles (see Section 6.1). $N_\sigma = 2.3$ defines the voltage threshold. Explicitly, θ_{th} is (when electromagnetic or hadronic energy deposition dominates):

$$\Delta\theta_{th} = \sqrt{-2 \cdot \Delta\theta(\mathrm{max})_{\mathrm{em,had}}^2 \cdot \ln \frac{\mathrm{V}_{\mathrm{noise}}^{\mathrm{max}} \cdot \mathrm{N}_\sigma}{\mathrm{f}_{\mathrm{em,had}} \cdot \mathcal{E}^{(@1\mathrm{m})}{}_{\mathrm{max}}(\sin\theta_{\mathrm{v}} = 1) \cdot \mathrm{h}_{\mathrm{eff}}^{\mathrm{max}} \cdot \mathrm{B}}} \qquad (16)$$

When the electromagnetic and hadronic components of the shower are both non-negligible, then we find the angular threshold by stepping by increments of 0.5 $\Delta(\mathrm{max})\theta_{\mathrm{em}}$ (we could have chosen to step in either $\Delta(\mathrm{max})\theta_{\mathrm{em}}$ or $\Delta(\mathrm{max})\theta_{\mathrm{had}}$) away from the center of the Cerenkov cone. When the ray is $\Delta\theta$ from the center of the Cerenkov cone, the maximum

voltage observed at the antenna is derived as in Equation 14, but adding the electromagnetic and hadronic components (this time we use $\theta_v = \theta_c + \Delta\theta$ since we are not inverting the equation in this case):

$$V_{rx} = \left[f_{em} \cdot \exp\left(-\frac{1}{2} \cdot \frac{\Delta\theta^2}{\Delta\theta(\max)^2_{\rm em}} \right) + \mathrm{f_{had}} \cdot \exp\left(-\ln 2 \cdot \frac{\Delta\theta^2}{\Delta\theta(\max)^2_{\rm had}} \right) \right] \cdot \mathcal{E}^{(@1\mathrm{m})}{}_{max}(\theta_v = \theta_c + \Delta\theta) \cdot h^{max}_{eff} \cdot B \quad (17)$$

Here, V_{rx} is the maximum voltage seen at the antenna for a given θ, and all of the variables in Equation 17 are found as described for the previous case above. The angular threshold θ_{th} is the angle at which V_{rx} falls below $V^{max}_{noise} \times N_\sigma$.

4.2 Finding Earth/Ice Entrance Points for the Neutrino

Finding the entrance point for the neutrino $\vec{r}_{in}$, given $\vec{p}_\nu$ and $\vec{x}_{int}$ is a simple geometry problem. Define:

$$a \equiv p \times \cos\theta + \sqrt{R_e^2 - p^2 \cdot \sin^2\theta} \quad (18)$$

where θ is the angle between $\vec{p}_\nu$ and $\vec{x}_{int}$. Then, the entrance point for the neutrino is:

$$\vec{r}_{in} = \vec{x}_{int} - a \times \vec{n}_\nu. \quad (19)$$

The quantity inside the square root is negative for events where the interaction occurred above sea level and the neutrino is down-going. These events are treated separately and the entrance point is found iteratively. First, the elevation $h^{(0)}_{int}$ is found at the latitude and longitude where the interaction occurred, and then R_e in the above equation is replaced with $R_e + h^{(0)}_{int}$ and a first guess at an entrance point is found. Then the elevation at that latitude and longitude, $h^{(1)}_{int}$, is found and R_e is replaced with $R_e + h^{(1)}_{int}$. After four iterations, all but a few percent of the events have converged with a difference between entrance points by successive iterations being less than the interaction length for that energy.

4.3 Balloon and Antenna Positions and Orientations

The balloon sits at an altitude of 37 km at 80° S latitude. The position of the balloon in longitude is selected at random for *each* neutrino generated.

The payload design of interest may be selected in the input file. For each design, the antennas are given the correct orientation in ϕ and inclination in θ at the right radius from the payload axis, spaced appropriately along the vertical axis. The input file also asks for the number of layers to be included. If the SMEX payload design has been chosen, and the user sets the number of layers to be 3, then only the top 3 layers of antennas out of the 4 layers in that design are included in the simulation. This is so that the nadirs can easily be turned on and off.

5 Ice

5.1 Attenuation in the Ice

The user may set the attenuation length for radio in ice to be a constant value (currently 700 m, on the conservative side), or a depth-dependent attenuation length based on (wu-fan.measurements performed at Ross Ice Shelf and the South Pole. [3]) The latter is the default. Fenfang Wu, working with David Goldstein, incorporated this feature into the code.

(wufan. i. For Ice Shelf, we just treat Ronne Iceshelf the same way as Ross Ice Shelf and we find the average attenuation length for upward direct rays:

$$\langle L\rangle = \frac{\int_{-d_{int}^{eff}}^{0} 1250 * 0.38 * 0.08886 * \exp(-0.048827 * (225.67460 - 86.517596 * \log_{10}(\mathrm{x} + 848.870)))dx}{d_{int}^{eff}} \tag{20}$$

For reflected rays which are first downward and then upward, the average attenuation length:

$$\langle L\rangle = \frac{\int_{-d_{int}^{eff}}^{-d_{max}^{eff}} 1250 * 0.38 * 0.08886 * \exp(-0.048827 * (225.67460 - 86.517596 * \log(\mathrm{x} + 848.870)))dx + \int_{-d}^{0}}{2 * d_{max}^{eff} - d}$$

(21)

where the interaction performed from the height of the interaction relative to the surface $x = -d_{int}^{eff}$ (a negative number) to the surface ($x = 0$). Since the measurements were only carried out to a depth of 420 m at Ross Ice Shelf, an effective maximum depth and effective interaction depth are utilized given by:

$$d_{int}^{eff} = d_{int} \qquad (d_{max} < 420\mathrm{m}) \tag{22}$$

$$d_{max}^{eff} = d_{max} \qquad (d_{max} < 420\mathrm{m}) \tag{23}$$

$$d_{int}^{eff} = d_{int} \times \frac{420\mathrm{m}}{d_{max}} \qquad (d_{max} > 420\mathrm{m}) \tag{24}$$

$$d_{max}^{eff} = 420 \qquad (d_{max} > 420\mathrm{m})(\mathrm{wufan}) \tag{25}$$

ii. For other places on Antarctica,

For direct rays which is always upward, the average attenuation length:

$$\langle L\rangle = \frac{\int_{-d_{int}^{eff}}^{0} 1250 * 0.08886 * \exp(-0.048827 * (\exp(\frac{1214.15-\mathrm{x}}{1004.40}) - 55.5889))dx}{d_{int}^{eff}} \tag{26}$$

For reflected rays which are first downward and then upward, the average attenuation length:

$$\langle L\rangle = \frac{\int_{-d_{int}^{eff}}^{-d_{max}^{eff}} 1250 * 0.08886 * \exp(-0.048827 * (\exp(\frac{1214.15-\mathrm{x}}{1004.40}) - 55.5889))dx + \int_{-d_{max}^{eff}}^{0} 1250 * 0.08886 * \exp}{2 * d_{max}^{eff} - d_{int}^{eff}} \tag{27}$$

Here the measurements were only carried out to a depth of 2810 m, so:

$$d_{int}^{eff} = d_{int} \qquad (d_{max} < 2810\mathrm{m}) \tag{28}$$

$$d_{max}^{eff} = d_{max} \qquad (d_{max} < 2810\mathrm{m}) \tag{29}$$

$$d_{int}^{eff} = d_{int} \times \frac{2810\mathrm{m}}{d_{max}} \qquad (d_{max} > 2810\mathrm{m}) \tag{30}$$

$$d_{max}^{eff} = 2810 (d_{max} > 2810\mathrm{m}) \tag{31}$$

In the above formulas, d_{max} is the real maximum depth of the ice at the longitude and latitude position where the interaction occurred. d_{int} is depth of the interaction (a positive number). wufan) Then, this attenuation is imposed on the signal:

$$E \to E \cdot e^{-D/\langle L\rangle}. \tag{32}$$

where E is the electric field of the signal and D is the distance that the RF signal travels through the ice. D is the magnitude of the difference between $\vec{x}_{int}$ and the point where the RF signal exits the ice, the latter found by the method described in Section 5.3. (wufan.For reflect rays, we use 10 percent of power reflection rate, so:

$$E \to 0.316227766E \cdot e^{-D/\langle L\rangle}. \tag{33}$$

)

5.2 Index of Refraction

The index of refraction of deep ice n_{ice} is taken as 1.79, and at the surface the index of fraction n_{surf} is 1.325. At depths shallower than 150 m is the firn, which is layers of packed

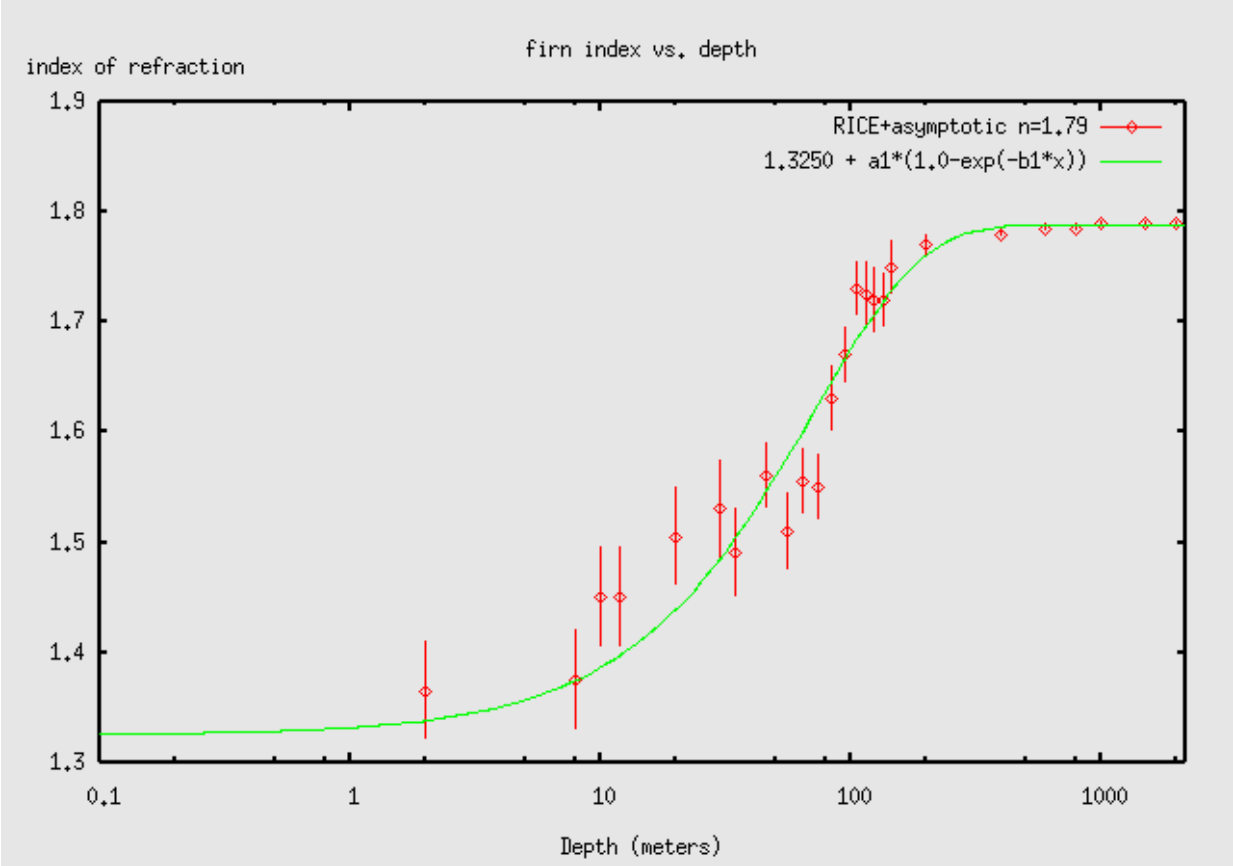

Figure 3: Fit to RICE data for index of refraction as a function of depth below the surface. Plot is from Peter Gorham.

snow. We use the following equation for the index of fraction n_{firn} as a function of altitude (h_{int}, a negative number, here in m) in the firn [1].

$$n(h_{int}) = 1.325 + 0.463251 \times e^{-0.140157 \times h_{int}} \tag{34}$$

This equation is a fit to the data measured by members of the RICE Collaboration. See figure 3.

5.3 Ray Tracing

We need to determine the path of the ray that emerges from the interaction point and arrives at the balloon's position (the distances between antennas on the payload are small enough to ignore compared to the distance between any interaction point and the balloon).

Our first guess for the RF exit point is the point on the ice surface that is directly radially outward from the interaction point. We call the vector from the earth's center (the origin of the coordinate system) to the RF exit point $\vec{r}_{exit,0}$ and we call the normalized vector from the interaction point to the RF exit point $\vec{n}_{refr,0}$. The surface normal at this exit point would also point radially away from the center of the earth were it not for the "tilt" at the surface. We take this into account by rotating the radial vector in the ϕ and θ directions to get the surface normal $\vec{n}_{surf,0}$. The magnitude of the rotation in each direction is the inverse tangent of the slope along that dimension determined from the difference in the altitudes of its two neighboring bins in latitude and longitude.

Once $\vec{n}_{surf,0}$ is found, its direction is randomized to account for surface "slopeyness." To each component of $\vec{n}_{surf,0}$ we add a number picked from a Gaussian distribution of width 0.012. Then, $\vec{n}_{surf,0}$ is normalized again.

Then, $\vec{n}_{e-b,0}$ is the vector running from the first guess RF exit point to the balloon's position.

Using $\vec{n}_{e-b,0}$, we arrive at our second guess for the direction of the ray in the ice $\vec{n}_{refr,1}$ using Snell's law, in its unfamiliar and not-so-appealing form

$$\vec{n}_{refr,1} = -\left(\frac{n_{air}}{n_{surface}}\cos\theta_i - \sqrt{1-\left(\frac{n_{air}}{n_{surface}}\sin\theta_i\right)^2}\right)\vec{n}_{surf,0} + \frac{n_{air}}{n_{surface}}\vec{n}_{e-b,0} \qquad (35)$$

to get the refracted ray at the surface (the top of the firn). Then, we use Snell's law again, replacing n_{air} with $n_{surface}$ and $n_{surface}$ with n_{depth} to get the refracted ray at the depth where the interaction occurred. This ray is called $\vec{n}_{refr,1}$. The value n_{depth} is found by the method described in Section 5.2.

Using this new direction for the RF in ice, we find a new exit position $\vec{r}_{exit,1}$ and a new exit-to-balloon direction, $\vec{n}_{e-b,1}$. (wufan.Here for reflect rays, we use the mirror interaction point to get the new exit position and a new exit-to-balloon directio because the exit rays looks like coming from the mirror interaction point.) Instead of finding a new $\vec{n}_{surf,1}$, however, we still use $\vec{n}_{surf,0}$ due to the slopeyness that was imposed. Finally, we do one last iteration and use Equation 35 twice again, changing subscripts on the RHS from $0 \rightarrow 1$, to find $\vec{n}_{refr,2}$, and from that deduce $\vec{r}^{exit,2}$, $\vec{n}_{surf,2}$, $\vec{n}_{e-b,2}$.

Figures 4 and 5 shows the difference between the exit points from successive iterations, showing that the method does converge.

5.4 Slopeyness

We take the surface normal at the longitude and latitude where the interaction occurs and randomize each component, allowing it to change by as much as 1.2%. This gives 0.01 rad

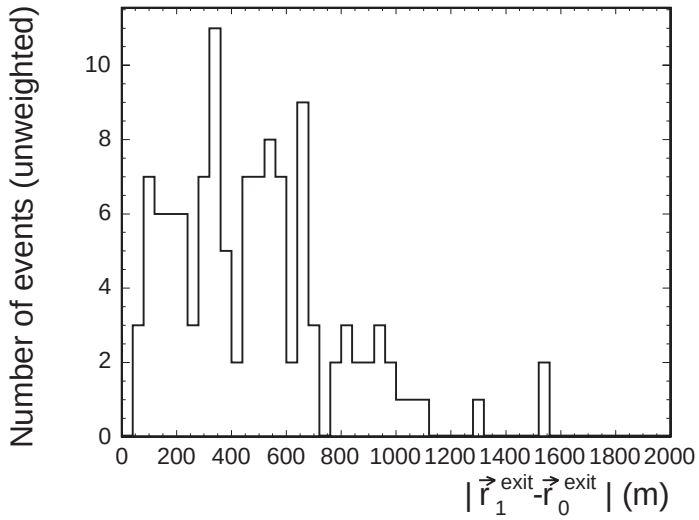

Figure 4: Difference in meters between RF exit points along the ice-air boundary from the first and second ray-tracing iterations.

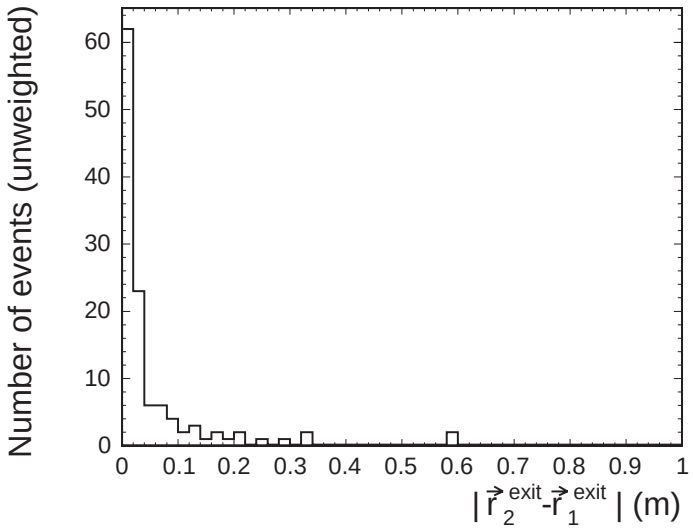

Figure 5: Difference in meters between RF exit points along the ice-air boundary from the second and third ray-tracing iterations.

as the mean magnitude of the slope.

5.5 Fresnel Factor

When the rays from the Cerenkov cone reach the ice-air boundary they just obey boundary conditions and thus the magnitude of the electric field is altered and the signal traverses the boundary [15]. This Fresnel factor, as it is called, for the "pokey" case is:

$$f_{\parallel,\perp} = \sqrt{\frac{\tan\theta_I}{\tan\theta_T}(1 - r_{\parallel,\perp}^2)} \tag{36}$$

where $r_\parallel$ is:

$$r_\parallel = \frac{\tan(\theta_I - \theta_T)}{\tan(\theta_I + \theta_T)}. \tag{37}$$

and $r_\perp$ is the Fresnel coefficient for the "slappy" case:

$$r_\perp = \frac{\sin(\theta_I - \theta_T)}{\sin(\theta_I + \theta_T)}. \tag{38}$$

For the pokey case, the polarization vector is perpendicular to the plane of incidence, and for the slappy case the polarization vector is in the plane of incidence. The general case is composed of both components.

After dividing up the electric field emerging from the ice into its "pokey" and "slappy" components, $E_\parallel^{ice}$ and $E_\perp^{ice}$, the electric field that emerges from the ice E_{air} is

$$E_{air} = \sqrt{\left(E_\parallel^{ice} \cdot r_\parallel\right)^2 + \left(E_\perp^{ice} \cdot r_\perp\right)^2} \tag{39}$$

We are in the process of verifying that the magnification (separate from the Fresnel coefficient) is also treated properly in our simulation.

6 Antenna Response

6.1 Noise

An antenna that sees only the sky will see noise due to the temperature of the sky (we take $T_{sky} = 15$ K) and the temperature of the front-end electronics ($T_{syst} = 200$ K). An antenna that points downward will see less sky and more ice ($T_{ice} = 240$ K). For a given antenna declination, we find the effective temperature by performing a weighted average of the power

seen by the antenna at each declination angle, taking into account the antenna beam widths. The effective temperature T_{eff} for a cant angle θ_{ant} is:

$$T_{eff} = \frac{\int_{-\pi}^{\theta_{horiz}-\theta_{ant}} (T_{sky} + T_{syst}) \cdot e^{-2 \cdot \ln 2 \cdot (\theta/\theta_0)^2} d\theta + \int_{\theta_{horiz}-\theta_{ant}}^{+\pi} (T_{ice} + T_{syst}) \cdot e^{-2 \cdot \ln 2 \cdot (\theta/\theta_0)^2} d\theta}{\int_{-\pi}^{+\pi} e^{-2 \cdot \ln 2 \cdot (\theta/\theta_0)^2} d\theta} \tag{40}$$

where θ_{horiz} is the declination at which the balloon at altitude 37 km sees the horizon 700 km away. Taking into account the earth's curvature, we find $\theta_{horiz} = \sqrt{(2 * h_b/g_b)} = 0.11\text{rad} \approx 6.2^\circ$ where $h_b = 37.0$ km is the altitude of the balloon and g_b is the radius of the geoid at the balloon's latitude. At 80°S, $g_b = 6357.7$ km.

Based on this calculation, an antenna canted by 10° sees an effective temperature of 338.8 K and an antenna canted by 55° an effective temperature of 428.3 K.

6.2 Trigger

We divide up the total bandwidth of the system (200 MHz to 1200 MHz) into four sub-bands whose central values are: 265, 435, 650 and 980 MHz and whose widths are: 130, 160, 250 and 370 MHz. A trigger channel is one polarization (left- or right- circularly polarized) of one antenna for in one sub-band in frequency.

The trigger in this simulation is the one described in Gary Varner's note [10]. The top two layers of eight antennas on the payload are combined into one layer of 16 antennas for the purpose of triggering. So, the trigger sees three layers of antennas: two layers of 16 antenns, and the third layer is the eight nadir antennas. At Level 1, an antenna passes the trigger if three out of 8 channels (2 polarizations, 4 bandwidth slices) surpass the threshold, which is $N_{sigma} = 2.3$ times the expected noise voltage for that channel. At Level 2, trigger channels are considered in groups of contiguous antennas, and the trigger is fired if enough antennas in that group pass the Level 1 trigger. For the top two trigger layers, there are 5 antennas in a group and at least 2 must pass. For the nadir antennas, the requirement is 2 out of 3. There is a separate trigger that considers nadir antennas only, and that requirement is 3 out of 3 contiguous nadir antennas is a group. At Level 3, either two different layers are required to have passed at Level 2, or the nadir-only Level 2 trigger must have fired. The noise voltage V_{noise} is chosen at random from a Gaussian distribution with a standard deviation equal to the expected noise for that channel's bandwidth and RF temperature.

The antenna parameters are inferred from the manufacturer's specifications for the antennas used in the Anita-lite flight. The manufacturer is Seavey Engineering Associates, Inc. and antenna used is the 0.3-1.5 GHz Dual Linear Polarized Quad Ridge Antenna Model 0312-810. The specs give the antenna gain for 5 values of frequency from 300 MHz to 1200 MHz and the beam width for the E-plane and H-plane, and for the vertical and horizontal polarization of each. We interpolate between these points to find the gains the beam widths

at the frequencies between those values given. For the region below 200 MHz, we use the values given in the specs for 300 MHz. Gains are all between around 8 and 12 dBi and are denoted G. The beam widths vary from around 35° to 65° are are denoted $b_E^h(\nu)$, $b_E^v(\nu)$, $b_H^h(\nu)$ and $b_H^v(\nu)$, where the subscripts and superscripts denote the horizontal and vertical polarizations in the E-plane and H-plane. At a given frequency ν, the effective height of the antenna is related to the gain by:

$$h_{eff}(\nu) = 2 \times \sqrt{\frac{G \cdot c^2}{4\pi \cdot \nu^2} \cdot \frac{Z_{rx}}{Z_{air}}} \tag{41}$$

where $Z_{air} = 377\ \Omega$ is the impedance of free space and $Z_{rx} = 50\ \Omega$ is the impedance of the antenna.

For a signal $F(\nu)$ incident on the i^{th} antenna at an angle θ_H off of the H-plane and an angle θ_E off of the E-plane, the 0^{th} polarization ($j = 0$) and 1^{st} polarization ($j = 1$) signal in the k^{th} sub-band from the antenna is:

$$V_{ijk} = \sum_{p=p_{min}(k)}^{p_{max}(k)} \frac{1}{\sqrt{2}} \cdot F(\nu_p) \cdot 0.5 \cdot h_{eff}(\nu_p) \cdot \Delta\nu \cdot c_j \cdot \exp(-\ln 2 \cdot \left[\left(\frac{\theta_{\rm E}}{{\rm b}_{\rm E}^{\rm j}(\nu_{\rm p})} \right)^2 + \left(\frac{\theta_{\rm H}}{{\rm b}_{\rm H}^{\rm j}(\nu_{\rm p})} \right)^2 \right]) \tag{42}$$

Frequency bins run across all four sub-bands between $\nu_1 = 200$ MHz and $\nu_2 = 1200$ MHz, so that $\Delta\nu = 10$ MHz, but the k^{th} sum is over frequency bins within the k^{th} sub-band, p_{min} to p_{max}. We take $c_0 = c_E$ and $c_1 = c_H$, where c_E (c_H) is the component of the incident ray parallel to the E-plane (H-plane) and perpendicular to the normal plane. If c_N is the component parallel to the normal plane and perpendicular to both c_E and c_H, then the vector (c_E, c_H, c_N) is a unit vector. The magnitudes of the left and right circularly polarized signals are each:

$$V_{i(L,R)k} = \sqrt{V_{i0k}^2 + V_{i1k}^2}. \tag{43}$$

7 Volume × Steradians

The water-equivalent $[V\Delta\Omega]$ is computed using the following formula:

$$[V\Delta\Omega] = V \times \frac{\rho_{ice}}{\rho_{H_2O}} \times 4\pi \times \frac{\Sigma w_i}{N} \times \frac{\sigma_{\rm SM}}{\sigma} \tag{44}$$

The variables are:

- V is the entire volume of Antarctic ice, computed by summing over all bins the product of the ice thickness and the cross-sectional area of the bin.

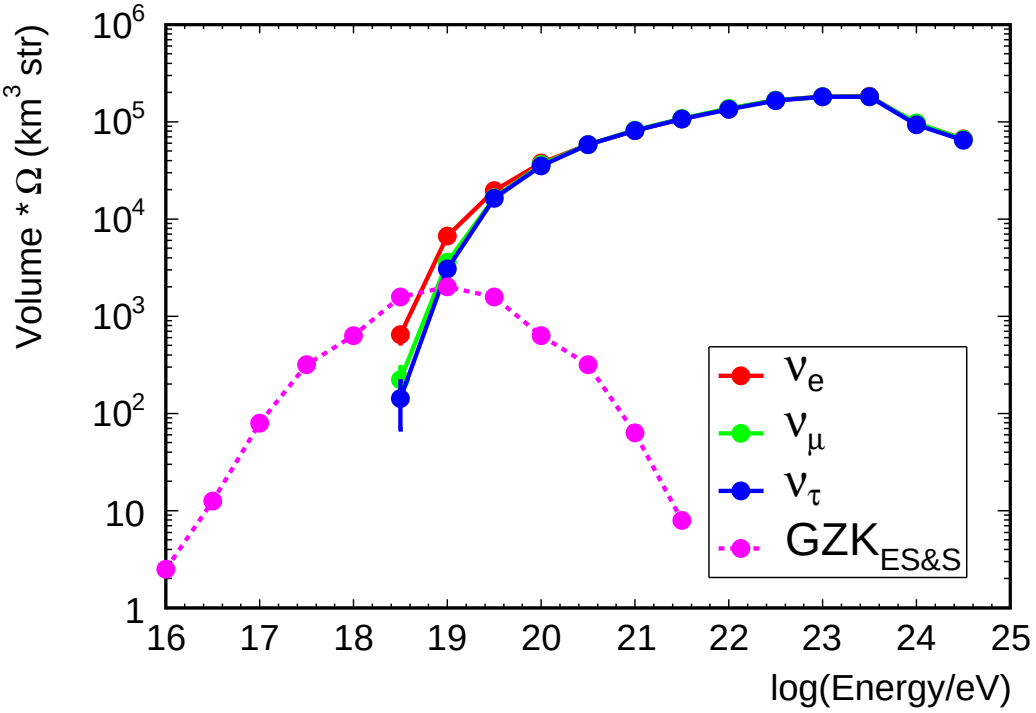

Figure 6: Effective Volume times steradians from this simulation. We also show the predicted GZK flux with a reasonable set of parameters from [5].

- ρ_{ice} and ρ_{H_2O} are the densities of ice and water, respectively.
- N is the number of neutrinos that the user asks to be generated.
- w_i is the weight given to each event, described in Section **??**.
- $\sigma_{\rm SM}$ is the Standard Model νN cross section
- σ is the νN cross section used for this run

Figure 6 shows the volume $\times$ steradians attained from this simulation.

7.1 Weighting the Events

In addition to accounting for phase space reduction described previously, we weight each event according to the probability that it interacted in the earth before it reached the ice.

As a neutrino moves through the earth, it encounters varying densities as it passes through layers of the earth's interior, and thus differing interaction lengths.

The probability that a neutrino interacts in the rock is:

$$w = \prod_{i=0}^{n} e^{-x_i/L_i} = \prod_{i=0}^{n} e^{-x_i\rho_i/\ell} = e^{\frac{1}{\ell}\sum_{i=0}^{n} x_i\rho_i} \tag{45}$$

where n is the number of layers the neutrino traverses. A "layer" can be the crust, the mantle, or one seven layers defined in Crust 2.0.

Then x_i is the distance the neutrino travels through the i^{th} layer in meters, ρ_i is the density of the i^{th} layer, L_i is the interaction length of that layer in meters, and ℓ is the interaction length in kg/m^2.

To find the column density of the chord in kg/m^2 (the sum $\sum_{i=0}^{n} x_i \cdot \rho_i$) traversed by the neutrino, we have two different options in the code, but describe the default method here.

The total chord length in kg/m^2 is calculated as follows. We first step in 50 m steps along the neutrino's path as it enters the earth through the crust, summing over $x_i\rho_i$ where x_i is the length of the i^{th} step and ρ_i is the density the layer that contains that step. We continue stepping until we are too deep to be in the earth's crust based on Crust 2.0. At each point, the depth along the neutrino's path is calculated relative to the height of sea level according to the geoid model. Next, the distance that the neutrino travels through the mantle is found through a simple geometrical calculation. The density of mantle is taken to be 3400 kg/m^2. The product of the path in the mantle and the mantle density is added to the sum. Then, we step through the remaining neutrino path to the interaction position, finishing the summation.

7.2 Phase Space Factor

The phase space factor d_i for the i^{th} event is the product of the phase space factor that comes about when we select the neutrino interaction position (d_i^{pos}) and the one that comes about when we select the neutrino direction (d_i^{dir}). Therefore, $d_i = d_i^{pos} \times d_i^{dir}$.

The position of the neutrino interaction is forced to be in the volume of ice that is within the horizon of the balloon. The balloon's longitudinal position along the 80° S latitude line is chosen at random for each event. The phase space factor d_i^{pos} is then just the total volume of ice in Antarctica divided by the volume of ice within the horizon for the i^{th} event. The volume of ice within the horizon is calculated once at the start of the program for 100 equally spaced balloon positions along its circular path. For each event, we take the pre-calculated volume for the balloon position that is closest to the balloon position for that event.

The neutrino direction is chosen such that the its Cherenkov cone lies close enough in solid angle to the interaction-to-balloon line of sight that it is possible that the event is observable under the most optimistic of circumstances, as described in Section 4.1. Since the direction for the i^{th} neutrino is chosen from the intersection of a cone of width $2\sin\theta_{thi}$ and a unit sphere, the corresponding phase space factor is:

$$d_i^{dir} = \frac{4\pi}{\sin\theta_c \cdot 2\sin\theta_{thi} \cdot 2\pi} \tag{46}$$

8 Cross Section Enhancements

8.1 Error on the Effective Volume × Steradian

Since $[V\Delta\Omega]$ is derived from a sum of weights, the statistical error is non-trivial. Imagine we histogram all of the weights that are summed into M equally spaced bins between 0 and 1. Then, the total number of events that pass our Monte-Carlo simulation (which only differs from $[V\Delta\Omega]$ by a constant) is given by:

$$\sum_{i=0}^{M} f_i \cdot w_i \tag{47}$$

where f_i is the number of events fall in the i^{th} bin centered on weight w_i. We define ϵ to be the error on f_i. When $f_i < 20$, we use the appropriate Poisson errors from [8], keeping track of asymmetric errors. When $f_i > 20$, $\epsilon = \sqrt{f_i}$. Then, the total error on the sum of weights is:

$$\sqrt{\sum_{i=0}^{M} (\epsilon_i \cdot w_i)^2} \tag{48}$$

9 Coding

9.1 Random Number Generation

The `gRandom` variable is a global variable set up by Root that points to a random number generator instance of the type TRandom3. At the beginning of the program, we set gRandom to an instance of TRandom3 with a seed that we set to a constant. One can change the value of that seed to a different constant through an option in the input file. You may want to use this option if, for example, you want to simultaneously run multiple jobs with different seeds and be able to combine the results for increased statistics.

For the sake of repeatability, we set the random number seed to a constant instead of, for example, setting it to the current time as is often done. We would like to be able to get identical outputs for equivalent code with the same inputs.

10 Future Improvements

The authors are aware that there are many effects that still need to be included and improvements that need to be made for this simulation. These include:

- Surface roughness needs to be treated properly.
- Double-bang taus need to be included.

References

[1] Peter Gorham, personal communication.

[2] Bassin, C., Laske, G. and Masters, G., The Current Limits of Resolution for Surface Wave Tomography in North America, EOS Trans AGU, 81, F897, 2000, http://mahi.ucsd.edu/Gabi/rem.html.

[3] Anita SMEX proposal, www.phys.hawaii.edu/∼gorham/ANITA/AnitaCSR.pdf, p. 15.

[4] Eidelman et al., Physics Letters B592, 1 (2004)

[5] R. Engel, D. Seckel, T. Stanev, "Neutrinos from Propagation of Ultrahigh Energy Protons, Phys.Rev. D64:093010

[6] J. Alvarez-Muniz, R.A. Vazquez and E. Zas, "Calculation Methods for Radio Pulses from High Energy Showers," astro-ph/0003315.

[7] Ghandhi,Reno,Quigg,Sarcevic, hep-ph/9512364.

[8] Gary J. Feldman, Robert D. Cousins, Phys.Rev.D57:3873-3889,1998, physics/9711021.

[9] http://www.pol.ac.uk/psmsl/puscience/

[10] http://www.phys.hawaii.edu/∼idlab/publications/ANITA_GTM_Note.pdf

[11] Williams, Richard S. Jr. and Jane G. Ferrigno. Estimated present-day area and volume of glaciers and maximum sea level rise potential. Satellite Image Atlas of Glaciers of the World. US Geological Survey (USGS). http://pubs.usgs.gov/fs/fs133-99/gl_vol.html

[12] J. Alvarez-Muniz, Phys.Lett.B411:218-224 (1997) astro-ph/9706064.

[13] J. Alvarez-Muniz, Phys.Lett.B434:396 (1998) astro-ph/9806098.

[14] J. Alvarez-Muniz, *et al.*, Phys. Rev. D **74**, 023007 (2006) astro-ph/0512337.

[15] Dawn Williams, Ph.D. Thesis, http://www.physics.ucla.edu/∼dawnwill/